PCCP

Accepted Manuscript

ROYAL SOCIETY OF CHEMISTRY

www.rsc.org/pccp

Cite this: DOI: 10.1039/c0xx00000x

www.rsc.org/xxxxxx

ARTICLE TYPE

Spectral dependence of nonlinear optical properties of symmetrical octatetraynes with *p*-substituted phenyl end-groups

Agata Arendt,[a] Radosław Kołkowski,[b,c] Marek Samoć[b] and Sławomir Szafert[a]*

Received (in XXX, XXX) Xth XXXXXXXXX 20XX, Accepted Xth XXXXXXXXX 20XX

DOI: 10.1039/b000000x

Organic compounds containing conjugated carbon chains have been extensively investigated due to their interesting properties including nonlinear optical response. Polyynes are a group of compounds where the conjugation can be modified by proper selection of end-groups, enabling "control" and improvement of nonlinear effects. In this work we investigate three newly synthesized aryl end-capped octatetraynes, exhibiting strong nonlinear absorption and nonlinear refraction properties, which can be attributed to the presence of aryl end-groups with electron-withdrawing functional groups suitable for further extending of the conjugation. Nonlinear optical measurements were performed using *f*-scan (modified *Z*-scan) technique with a femtosecond laser system at various wavelengths in the visible and near-infrared range (540-1600 nm), revealing strong negative third-order nonlinear refraction (3NR) and two-photon absorption (2PA) below 600 nm and a noticeable three-photon absorption (3PA) at longer wavelengths. Results of the spectroscopic characterization and the crystallographic data of the investigated compounds are also presented.

Introduction

Carbon-rich compounds have been extensively explored during the last few decades. One class of such species are polyynes - compounds with a linear carbon chain consisting of alternating triple and single bonds between carbon atoms,[1,2] which can serve as a model for carbyne $(-C\equiv C-)_n$, a linear sp-hybridized allotrope of carbon that still remains a hypothetical material.[3,4] Oligoynes and polyynes are foreseen to be of interest for numerous applications, for instance as components for wires or switches in optoelectronic devices[5,6] or as component of co-crystals with conducting polymers.[7]

One of the main issues associated with such conjugated organic systems is their thermodynamic instability resulting from the tendency of the chains to cross-link, forming more stable graphene-like structures.[8] Stabilization of polyynes often involves the use of bulky end-groups, preventing the conjugated chains from approaching each other. The synthesis of polyynes with a variety of end-groups has been widely discussed in the literature. The first phenyl end-capped oligoyne was obtained by Glaser in 1869.[9] To date, the syntheses of polyynes with aryl,[10,11,12] bulky 'super trityl',[13] organometallic,[14,15] and silyl end-groups[16,17] were reported.

Third-order nonlinear optical (NLO) properties of polyynes have been extensively studied by means of theoretical modelling, addressing in particular the dependence of the cubic hyperpolarizability γ on the length of acetylenic chains. It has been found that increasing the number of repeated units in polyynes does not improve NLO properties as much as in similar series of polyenes.[18,19] Other computational studies concerned the effect of terminal groups, showing that phenyl end-capped polyynes exhibit superior γ values compared to other end-groups.[20] These findings suggested that moderately long aryl end-capped polyynes may be an optimal design concerning a compromise between the NLO properties, molecular weight of a molecule and its chemical stability.

Experimental confirmation of the theoretical predictions has been challenging due to the stability issues associated with polyynes. According to the best of our knowledge, only several size-selective experimental NLO studies on organic polyynes with various end-groups and chain lengths were successfully conducted. Tykwinski and co-workers studied nonlinear properties of triisopropylsilyl (TIPS)[16,17] and phenyl[21] end-capped polyynes using differential optical Kerr effect technique (DOKE), confirming higher NLO performance of the phenyl end-capped molecules. An unprofitability of the polyynic chain extension has been found in the experimental studies of organometallic ruthenium-terminated polyynes[22] and chromophore-terminated polyynes and polyenes,[19] performed by degenerate four-wave mixing (DFWM), however, in these studies the NLO activity was attributed more to the end-groups rather than polyynic chains. Very recently, NLO properties of a group of phenyl-end-capped polyynes were investigated using nanosecond *Z*-scan at the wavelength of 532 nm,[23] pointing out some additional phenomena such as molecular reorientation which can contribute to the unexpectedly large γ values observed when the measurements were performed using pulsed light sources of longer than picosecond pulse durations.

While in most cases the research has been directed towards the investigation of the chain length dependence of γ, spectrally

resolved studies have been rarely addressed. Such studies are crucial for correct interpretation of the results, providing better insight into molecular energy levels participating in multiphoton transitions. Some results obtained only at a single wavelength, such as the astonishingly rapid increase of the γ values with increasing acetylenic chains length in silyl end-capped polyynes[16,17] could be better explained in terms of a red shift of the resonantly enhanced multiphoton transition bands, which has been observed in the wavelength dependence of the cubic nonlinearity of platinum-terminated polyynes, measured by Samoć *et al*. using the *Z*-scan technique.[24] Moreover, investigation of the full spectral dependence may reveal higher-order NLO effects, which in the case of polyynes have not been yet investigated.

In this work we report on the synthesis of three new octatetraynes with electron withdrawing ester-substituted phenyl end-groups and present the results of spectrally-resolved investigation of NLO properties of these compounds, performed using the femtosecond *f*-scan technique.[25] The choice of the compounds seemed highly rational since no symmetrical systems with electron withdrawing substituents has yet been selected for the NLO measurements. Ester-substituted polyynes appeared reasonably stable and considering the enhancement of conjugation in such systems it was expected to give interesting results. Indeed, the measurements have revealed negative nonlinear refraction in the visible range and multiphoton absorption in the visible and near-infrared range. The observed values of γ are in the order of 10^{-32} esu, outperforming polyynes of similar size investigated in comparable experimental conditions.[24] These large values of γ can be attributed to the presence of the electron-withdrawing groups causing further extension of the conjugation. Additionally, we quantitatively describe the three-photon absorption (3PA) in the studied polyynes, which is performed for the first time to our best knowledge for this kind of organic compounds. We have also characterized the compounds using ^{1}H, ^{13}C NMR, and UV-Vis spectroscopy and HRMS. Solid-state structures for two of the studied compounds were also obtained.

Experimental section

Detailed synthetic procedures and characterization data for the investigated compounds can be found in Electronic Supplementary Information (ESI).† UV-Vis spectra were measured on a Cary 300 Bio spectrophotometer. The ^{1}H and ^{13}C NMR spectra were obtained using a Bruker Avance 500 MHz spectrometer. HRMS spectra were recorded using a spectrometer with TOF mass analyzer and ESI ion source. X-ray diffraction data were collected with the Xcalibur diffractometer with Ruby CCD camera (ω scan technique) equipped with an Oxford Cryosystem-Cryostream cooler at 100 K. The space groups were determined from systematic absences and subsequent least-squares refinement. Lorentz and polarization corrections were applied. The structures were solved by direct methods and refined by full-matrix, least-squares on F^2 using the SHELXTL Package.[26] Crystallographic data for the structures of **E1-C$_8$-E1** and **E2-C$_8$-E2** were deposited with Cambridge Crystallographic Data Centre as supplementary publication no. CCDC 1042757 and 1042758, respectively. These data can be obtained free of charge via www.ccdc.cam.ac.uk/data_request/cif.

Nonlinear optical properties were studied using the newly developed *f*-scan technique,[25] which is very similar to the well-known *Z*-scan,[27] except that the position of the sample (*z*) is fixed, whereas the focal length (*f*) of an electrically focus-tunable lens (Optotune EL-10-30 series) is changed. The light source used in *f*-scan measurements was a femtosecond laser system, tunable over the visible and near-infrared spectral range, consisting of an optical parametric amplifier (OPA, Quantronix Palitra) pumped by Quantronix Integra Ti:Sapphire regenerative amplifier (output wavelength 800 nm, pulse duration 130 fs, repetition rate 1 kHz). Femtosecond pulsed light source plays a crucial role in the proper determination of NLO parameters, removing any possible contribution of parasitic effects occurring at a different time scale, such as molecular reorientation which in case of anisotropically polarizable molecules may become a dominant process responsible for nonlinear refraction measured with pico- or nanosecond pulses.[28] The use of *f*-scan significantly shortened the time of a single measurement compared to *Z*-scan, minimizing the exposure of our potentially unstable compounds to the high-power pulsed laser radiation.[23] Moreover, the total duration of the whole series of measurements was reduced, lowering the risk of a long-term degradation of compounds. Detailed description of the *f*-scan technique, including the scheme of the experimental setup and the theoretical analysis, can be found in a recent publication.[25]

Results and discussion

Synthesis

The synthetic route for the preparation of the octatetraynes **E1-C$_8$-E1**, **E2-C$_8$-E2**, and **E3-C$_8$-E3** are outlined in Scheme 1. In the first step the Sonogashira coupling between bromo- or iodo-substituted aryl esters was carried out yielding silyl-protected phenylacetylenes. In the next step, 1-bromoacetylenes (**E1-E3-C$_2$Br**) were obtained with the use of NBS (*N*-bromosuccinimide) and $AgNO_3$/KF reaction system. The carbon chain elongation was attained *via* Cadiot-Chodkiewicz cross-coupling using $TMSC_2H$ in the presence of $Pd(PPh_3)_2Cl_2$/CuI catalyst and $NH(iPr)_2$ as a base.[29] The cross-coupling reactions were carried out in THF for 2-3.5 hours. The key step was the oxidative dimerization of trimethylsilyl-protected butadiynes (**E1-E3-C$_4$TMS**) that led to the aryl end-capped octatetraynes. Products **E1-C$_8$-E1** and **E2-C$_8$-E2** were obtained via Hay-Glaser homocoupling[30] with *in situ* deprotection using CuCl/TMEDA (*N*,*N*,*N*′,*N*′-tetramethylethylenediamine) catalytic system in the presence of TBAF as the deprotection agent, TMSCl (chlorotrimethylsilane) as the F^- ion scavenger, and O_2 as an oxidant.[31] The reactions were carried out in dry acetone for 20-22 hours. If the reaction time was too short, only products of deprotection of **E1-E3-C$_4$TMS** were observed. Our attempts to obtain compound **E3-C$_8$-E3** *via* Hay-Glaser coupling failed and therefore Eglinton homocoupling of deprotected butadiyne was performed yielding the target octatetrayne. Workup on flash column chromatography gave pure

Cite this: DOI: 10.1039/c0xx00000x

www.rsc.org/xxxxxx

ARTICLE TYPE

products with acceptable yields as presented in Scheme 1.

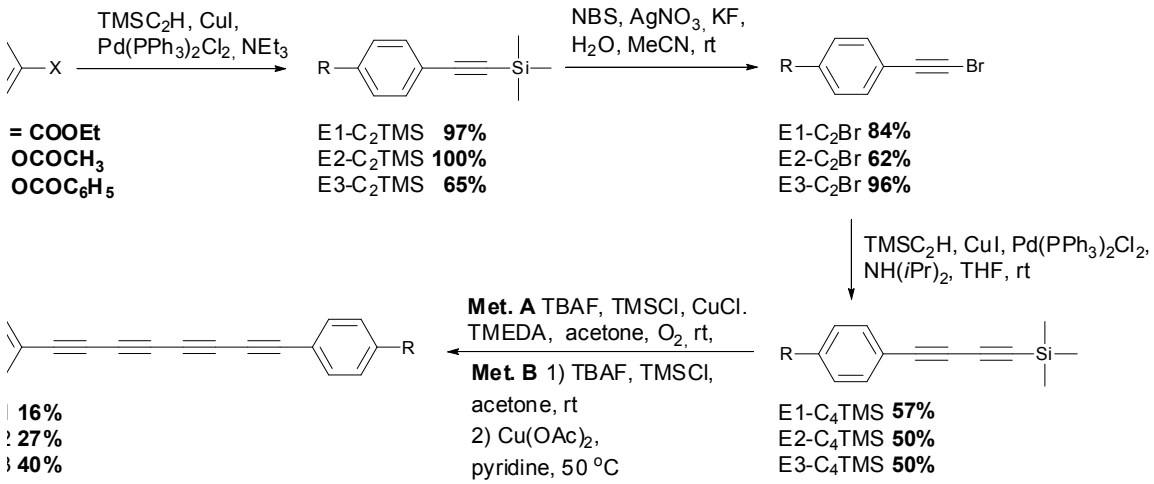

Scheme 1. Syntheses of the octatetraynes.

Crystal structures of octatetraynes

The crystal structures of **E1-C$_8$-E1** and **E2-C$_8$-E2** were determined and crystallographic data are presented in the Electronic Supplementary Information (ESI).† The monocrystals of **E1-C$_8$-E1** were obtained by slow evaporation of its acetone solution while **E2-C$_8$-E2** was crystallized from DCM (dichloromethane). **E1-C$_8$-E1** crystallized in P-1 space group, whereas **E2-C$_8$-E2** in C2/c space group. In both cases only half of the molecule resides in the asymmetric unit and the whole molecule is generated by symmetry operations.

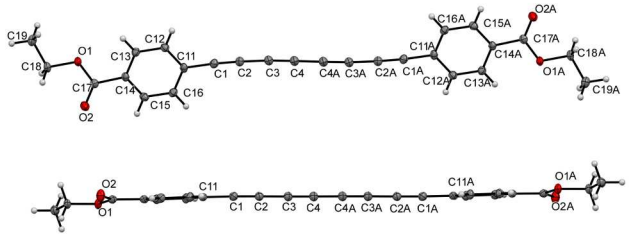

Figure 1. Molecular structure of **E1-C$_8$-E1.**

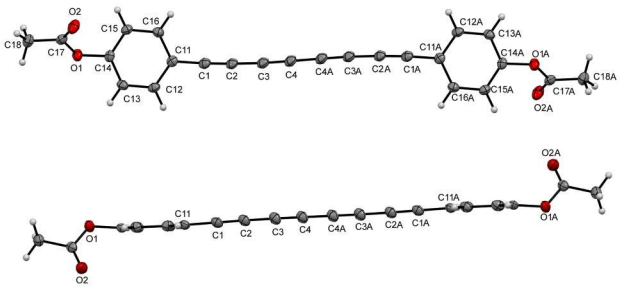

Figure 2. Molecular structure of **E2-C$_8$-E2**.

Table 1. Interatomic distances and angles for **E1-C$_8$-E1** and **E2-C$_8$-E2.**

	E1-C$_8$-E1	**E2-C$_8$-E2**
Interatomic distances [Å]		
C11—C1	1.4340(16)	1.431(2)
C1—C2	1.2060(17)	1.201(2)
C2—C3	1.3631(17)	1.362(2)
C3—C4	1.2108(17)	1.207(2)
C4—C4A^{i,ii}	1.363(2)	1.360(3)
O1—C17	1.4537(14)	1.3585(18)
O2—C17	1.2084(14)	1.1940(19)
C11—C11A dist	11.757	11.746
C11—C11A sum	11.791	11.762
% contraction	0.29	0.14
C1—C1A dist	8.913	8.895
C1—C1A sum	8.923	8.900
% contraction	0.11	0.06
Interatomic angles [°]		
C2—C1—C11	175.08(12)	177.11(17)
C1—C2—C3	177.07(12)	177.71(17)
C4—C3—C2	176.48(13)	177.20(17)
C3—C4—C4A^{i,ii}	179.49(17)	179.5(2)
O2—C17—O1	176.48(13)	123.44(15)
C17—O1—C14	112.73(10)	119.95(12)
O2—C17—C14	124.04(11)	-
O2—C17—C18	-	126.40(15)
Av. Angle	177.03	177.88

symmetry codes for: **E1-C$_8$-E1** (i) −x+2, −y+1, −z; **E2-C$_8$-E2** (ii) −x+1, −y+1, −z.

As presented in Figures 1-2 the molecules of **E1-C$_8$-E1** and **E2-C$_8$-E2** are almost ideally planar (the angles between the phenyl rings are 0° for both compounds due to the symmetry), with carbon atoms from the chain being no further than 0.160 and 0.112 Å out of the planes of phenyl substituents for **E1-C$_8$-E1** and **E2-C$_8$-E2**, respectively. Such geometry creates very favourable conditions for a strong conjugation across the entire molecule. In the structure of **E1-C$_8$-E1** the bond lengths within the carbon chain are 1.206(17) Å and 1.2108(17) Å for the triple bonds C1≡C2 and C3≡C4 and 1.3631(17) Å and 1.363(2) Å for the single bonds C2—C3 and C4—C4A, and they are similar to those in **E2-C$_8$-E2** and other tetraynes.[2,31,32] The polyyne carbon chains are only a little distorted from linearity with low contraction coefficients as described in Table 1.

Packing motifs and reactivity implications

The two structures crystallize in triclinic (P-1, **E1-C$_8$-E1**) and monoclinic (C2/c, **E2-C$_8$-E2**) systems. As a consequence, molecules of **E1-C$_8$-E1** form one set of parallel chains, while **E2-C$_8$-E2** are packed to form two non-parallel sets of parallel chains forming an angle of 13.9°. Figure 3 and 4 show packing diagrams for **E1-C$_8$-E1** and **E2-C$_8$-E2**.

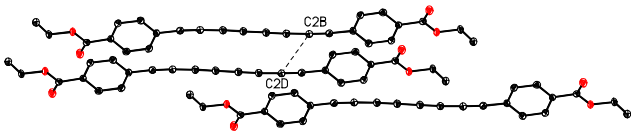

Figure 3. Packing diagram for **E1-C$_8$-E1** with the shortest chain–chain distance of 3.854 Å for C2B–C2D.

The closest chain-chain separation was then analyzed. As defined earlier,[2] we approximate the closest chain-chain distance as the closest carbon-carbon distance from two neighboring carbon chains. Accordingly, the nearest chains with parallel orientation for **E1-C$_8$-E1** are only 3.854 Å apart and this separation is slightly larger than a sum of the van der Walls radii (3.56 Å) and is analogous to that found for TMS(C≡C)$_4$TMS (3.853 Å).[33]

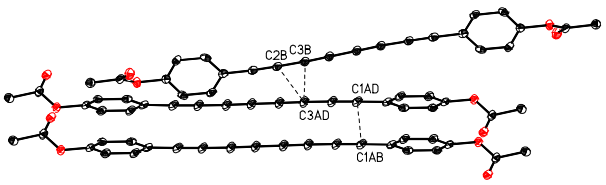

Figure 4. Packing diagram for **E2-C$_8$-E2** with the shortest chain–chain distances for parallel and non-parallel neighbors. The distances [Å] are: C2B–C3AD, 3.780; C3B–C3AD, 3.742; C1AD–C1AB, 3.863.

Table 2. Packing parameters for **E1-C$_8$-E1** and **E2-C$_8$-E2**.

Compound	**E1-C$_8$-E1**	**E2-C$_8$-E2**
chain-chain contact (Å, parallel)	3.854	3.863
ϕ (°)[2]	67.8	83.0
offset distance (Å)[2]	1.456	0.471
fractional offset	0.12	0.04
angle between nonparallel chains (°)	-	13.9
chain-chain contact (Å, nonparallel)	-	3.742

Despite the different space group, the shortest distance for **E2-C$_8$-E2** is almost identical (3.863 Å) to that of **E1-C$_8$-E1,** which is the consequence of a similar size of the end-group. Additionally, for **E2-C$_8$-E2** the chain-chain distance between non-parallel chains is even shorter than that between parallel chains and reaches 3.742 Å.

The 1,n-topochemical polymerization is one of the most important transformations that can take place in case of organic polyynes.[34] The geometric requirements for such process for tetraynes (1,8-polymerization) are fulfilled when the nearest parallel chains are separated by ca. 3.5 Å and ϕ angle is close to 21°. Searching for such values, it can easily be noticed (see Table 2) that there is no good candidate for 1,8-polymerization among the investigated compounds and both structures present more ladder type architectures (ϕ = 67.8° and 83.0°; for ideal ladder type ϕ = 90°) with a potential for 1,2 process.

UV-Vis Spectra

The UV absorption spectra of the octatetraynes are presented in Figure 5 and summarized in Table 3. Samples were prepared by dissolving the compounds in DCM with concentrations presented in Table 4. The UV-Vis spectra were measured in the 225-800 nm range (at intervals of 1 nm) however the absorption bands are observed only up to 425 nm.

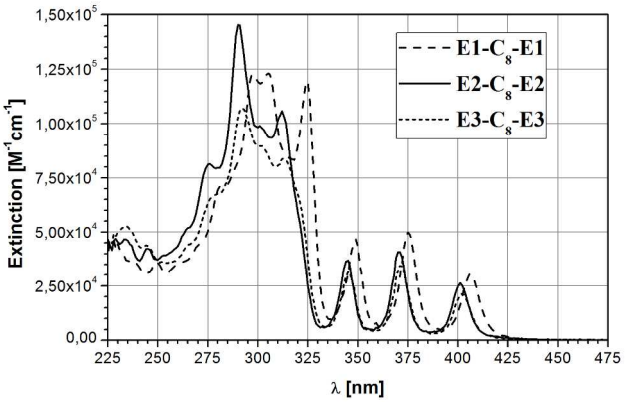

Figure 5. UV-Vis extinction spectra of the octatetraynes.

Table 3. Selected spectral data for octatetraynes.

	Region 1	**Region 2**
	λ_{max} [nm], ε [M^{-1} cm^{-1}]	λ_{max} [nm], ε [M^{-1} cm^{-1}]
E1-C$_8$-E1	306 (120000)	407 (30000)
E2-C$_8$-E2	290 (150000)	401 (27000)
E3-C$_8$-E3	293 (110000)	402 (21000)

The most intense absorption peaks (λ_{max}) are observed within 275-335 nm wavelength region. Narrow absorption peaks observed near 350, 370 and 400 nm are very similar for all the compounds due to the analogous length of the polyyne chain. Such spectra are characteristic for aryl-end-capped polyynes.[10,12] The highest molar absorptivity was observed for **E2-C$_8$-E2** (ε = 150000 M^{-1} cm^{-1} for λ = 290 nm) and the values of the molar absorptivities are comparable to the octatetraynes with other end-groups.[21]

Table 4. The sample concentration for UV-Vis spectra and nonlinear optical measurements.

	UV-Vis spectra	Nonlinear optical measurements
E1-C_8-E1	$5.1 \cdot 10^{-6}$ M	$4.4 \cdot 10^{-2}$ M
E2-C_8-E2	$4.1 \cdot 10^{-6}$ M	$4.8 \cdot 10^{-2}$ M
E3-C_8-E3	$4.6 \cdot 10^{-6}$ M	$1.0 \cdot 10^{-2}$ M

Nonlinear optical measurements

f-scan measurements were performed at different wavelengths in the spectral range of 540-1600 nm. All the compounds were dissolved in DCM forming transparent solutions of relatively high concentrations, as specified in Table 4. The solution of **E3-C_8-E3** could be obtained only with slightly lower concentration due to some stability and solubility problems. Each investigated solution was placed in a 1 mm-thick glass cuvette, and the transmitted intensity of a focused laser beam passing through the cuvette was recorded simultaneously in closed aperture and open aperture configurations as a function of the focal length *f* (which was then recalculated to *z*, that is the position of the sample with respect to the focus).

In addition to the cuvettes containing solutions of octatetraynes in DCM, which will be referred to as *samples*, each measurement included also three references: (1) empty space (required in closed aperture *f*-scan), (2) 4.66 mm-thick silica glass plate and (3) a cuvette containing pure solvent (DCM). The first reference is used to "correct" the closed aperture *f*-scan curves, so that the line-shape resembles the usual *Z*-scan data.[25] The second and third references are needed to calibrate the light intensity (making use of the known nonlinear refractive index of fused silica) and to calculate the nonlinear optical parameters referring to the pure solute[35] (pure octatetrayne). In addition, each open aperture *f*-scan curve of the sample is divided by the open aperture curve of the solvent (third reference), in order to remove any possible contribution of the nonlinear absorption of the solvent, as well as to get rid of the artefacts which may be present in both sample and solvent measurements.

The experiment at a given wavelength consisted of a sequence of three consecutive measurements, and the series of measurements at different wavelengths in the 540-1600 nm range was repeated after several days under slightly different experimental conditions (different laser power and beam diameter). The error of the determined NLO parameters is estimated based on the statistics, depending on the repeatability of the results (when the results were poorly repeatable, the error was larger).

The values of the real and imaginary parts of the cubic hyperpolarizability γ, corresponding to third-order nonlinear refraction (3NR) and two-photon absorption (2PA), respectively, are plotted in Figure 6. All the investigated compounds are found to exhibit strong third-order NLO properties: 2PA and negative 3NR are observed in the 540-580 nm spectral range, which roughly corresponds to the doubled wavelength of the peaks in the main one-photon UV absorption band. It needs to be mentioned here, that, due to the centrosymmetric character of the compounds, exact correspondence between the one-photon and two-photon spectra is not expected, the one-photon transitions being allowed to states of *ungerade* character and the two-photon transitions to *gerade* states. However, because of the presence of a large number of possible electronic excited states as well as to possible deviations from centrosymmetry, the rough coincidence of the appropriate wavelength ranges is not unexpected. More detailed understanding of the 2PA mechanisms would require identification of the electronic transitions involved in this process, which could be possible by quantum chemical calculations supported by proper analysis tools.[36]

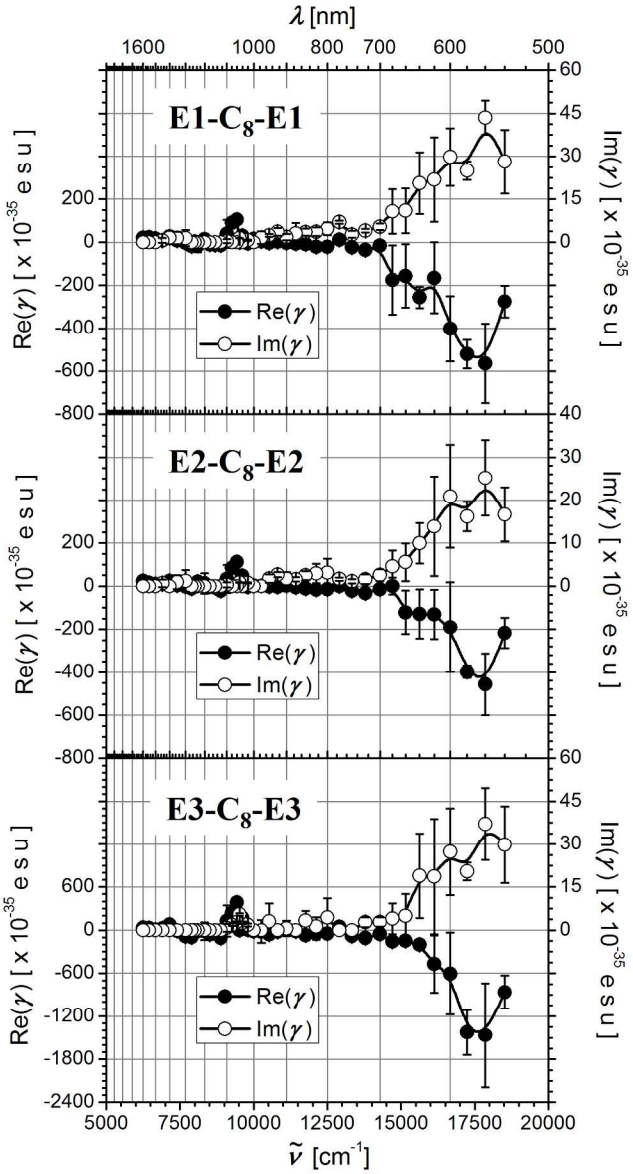

Figure 6. Dispersion of the cubic hyperpolarizability γ, real (filled circles) and imaginary part (empty circles), of the investigated octatetraynes, obtained using *f*-scan. For wavelengths above 620 nm the Im(γ) values account also for the higher order nonlinear effects.

The values of the relevant NLO parameters were extracted by fitting the experimental data (silica, solvent and samples) using

appropriate theoretical curves based on the *f*-scan modification of the theory given by Sheik-Bahae *et al.*[27] Representative closed aperture and open aperture *f*-scan traces at 560 nm for all three investigated samples are shown in Figure 7, together with the theoretical fits.

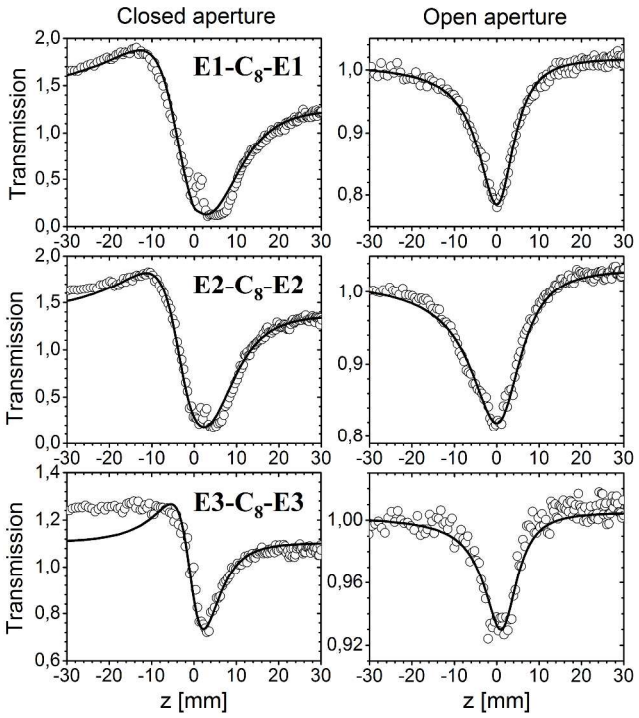

Figure 7. Representative *f*-scan traces of the investigated octatetraynes at 560 nm: experimental data (empty circles) fitted by theoretical curves (solid lines). Left: closed aperture curves involving negative 3NR accompanied by 2PA. Right: open aperture curves exhibiting optical limiting behaviour due to 2PA. The asymmetric shape of the curves (compared to traditional *Z*-scan) is a peculiar feature of *f*-scan and is fully accounted for by the theoretical model.

As for organic compounds of relatively low molecular weight (394.42 for **E1-C$_8$-E1**, 366.37 for **E2-C$_8$-E2** and 490.50 for **E3-C$_8$-E3**), the magnitudes of the obtained NLO parameters can be considered as very high. The effect of negative 3NR in all studied octatetraynes in the spectral range of 540-580 nm was so strong that it surpassed the positive 3NR of the solvent and the cuvette glass, causing inversion of the closed aperture curve (exchange of the peak and valley positions along the *z* axis). For example, the nonlinear phase shift $\Delta\Phi_0$ measured in the sample **E1-C$_8$-E1** (cuvette containing DCM solution of this compound) was equal -5.24 rad, whereas the values of $\Delta\Phi_0$ equal 0.88 rad and 1.34 rad were obtained under exactly the same experimental conditions for the silica plate and the cuvette with pure DCM, respectively. Taking into account the concentration of the solutions, the values of Re(γ) at the spectral maximum (around 560-580 nm) exceed -5×10^{-33} esu for **E1-C$_8$-E1**, -4×10^{-33} esu for **E2-C$_8$-E2**, and -1.4×10^{-32} esu for **E3-C$_8$-E3**. At the same time, the magnitude of Im(γ) varies in the range from 1 to 5×10^{-34} esu, that is one order of magnitude lower than Re(γ). Based on these results one may expect that organic compounds similar to the investigated ones could be promising for efficient optical switching, which requires the merit factor $|\mathrm{Re}(\gamma)/\mathrm{Im}(\gamma)|$ to be greater than 4π.[37] The highest values of this factor are found at 580 nm: $|\mathrm{Re}(\gamma)/\mathrm{Im}(\gamma)| > 20$ in **E1-C$_8$-E1** and **E2-C$_8$-E2**, and $|\mathrm{Re}(\gamma)/\mathrm{Im}(\gamma)| > 50$ in **E3-C$_8$-E3**. Molecular engineering of such compounds, aiming for optimization of the NLO performance in the useful (telecom) spectral range is a promising challenge for future research work.

Table 5. Comparison of Re(γ) values of different polyynes reported in the literature and in the present work.

triple bonds	end-group	$\lvert\gamma\rvert\times10^{35}$ esu	λ nm	sol-vent	tech-nique	Ref
4 10	Pr_3Si^i	1.25 ± 0.21 64.6 ± 2.7	800	THF	DOKE	16, 17
4 8	Ph	4.9 ± 1.8 58.8 ± 3.6	800	THF	DOKE	21
4 8	Ru_2	25000 ± 4000 18000 ± 3000	532	tolu-ene	DFWM	22
2 4	Ph	17000 130000	532	meth-anol	*Z*-scan	23
4 12	Pt	320 ± 80 7500 ± 1200	590 520	DCM	*Z*-scan	24
4 4 4	'E1' 'E2' 'E3'	520 ± 70 400 ± 30 1400 ± 300	580	DCM	*f*-scan	this work

Although direct comparison between the values of the real part of the second hyperpolarizability γ obtained using different techniques such as *Z*-scan, DOKE and DFWM may be erroneous, we find it appropriate to set together and discuss the values obtained in our work and the values determined in other research groups for similar compounds. It is done in Table 5, taking into account polyynes of the same number of triple bonds (4) as well as the longest polyynes studied in a given work (with an exception of Ref. 23, where polyynes up to 4 triple bonds were studied). Our results fall in between the relatively small magnitudes of γ reported in Ref. 16, 17 and 21, and the significantly larger values reported in Ref. 22 and 23. As already mentioned, low γ values of silyl and phenyl end-capped polyynes measured at 800 nm are probably a result of an off-resonant character of the NLO phenomena at this wavelength. On the other hand, results presented in Ref. 22 and 23 were obtained using nanosecond light sources, which makes the NLO measurements susceptible to contributions of parasitic phenomena such as molecular reorientation. In view of the above incompatibility issues, our results can be directly compared only with the work presented in Ref. 24. Indeed, the values of γ appear comparable, and the polyynes investigated in our work seem to slightly outperform compounds of similar polyynic chain lengths terminated by organometallic moieties.

In the wavelength range of 600-680 nm the results were more

ambiguous, large discrepancies being found between different series of measurements, leading to relatively large errors of the determined third-order NLO parameters. Analysis of the results led to the conclusion that part of the discussed spectral range is probably a region of spectral overlap and interplay between the NLO phenomena of different order. In particular, both two- and three-photon (3PA) processes may contribute to the resultant nonlinear absorption behaviour of the samples. This makes the values of the effective cubic hyperpolarizability (γ) dependent on the laser intensity, in a manner that is difficult to predict, as the relative contribution of different nonlinear absorption processes cannot be easily assessed.

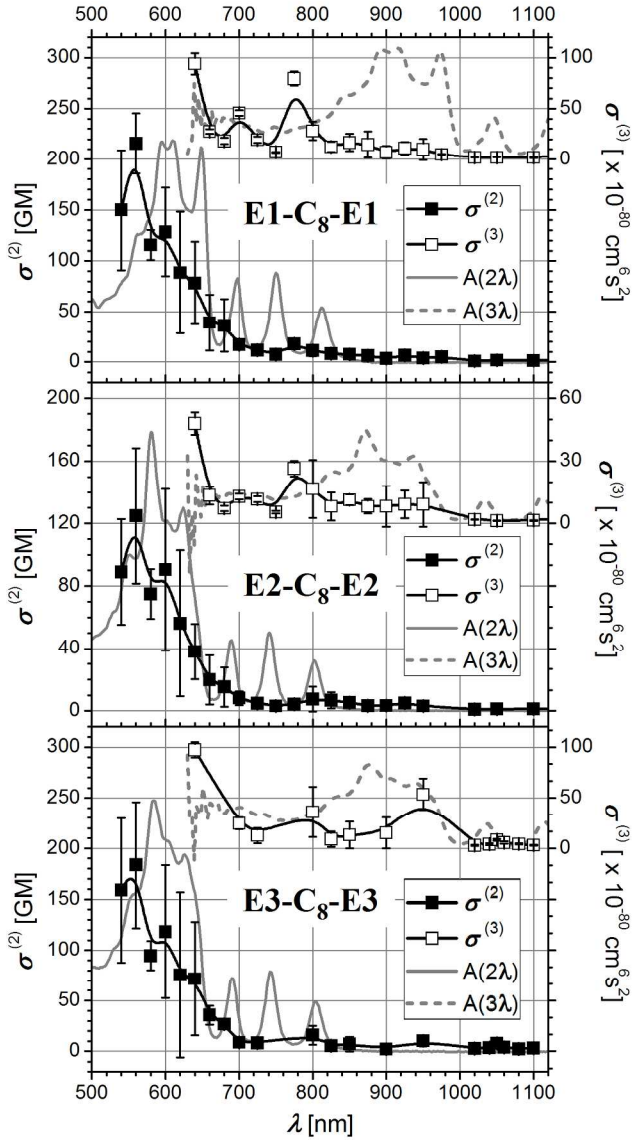

Figure 8. Dispersion of 2PA and 3PA absorption cross-sections $\sigma^{(2)}$ and $\sigma^{(3)}$ (black and white squares, respectively), superimposed with UV-Vis spectra plotted as a function of doubled and tripled wavelength (grey solid and dashed lines). The values of $\sigma^{(2)}$ may be affected by the contribution of 3PA above 580 nm. At longer wavelengths, the values of $\sigma^{(2)}$ and $\sigma^{(3)}$ may be affected by the contribution of 4PA (above 825 nm), and additionally by 5PA (above 1000 nm).

In addition, the possible instability of the samples cannot be excluded – one should be concerned that chemical changes, such as cross-linking of the polyynic chains, could have occurred during the measurements, affecting to some extent the NLO properties.[23] However, we presume that such effects are rather weak, as the NLO parameters in the 540-580 nm range were rather well reproducible during different series of measurements. The occurrence of 2PA and 3PA is summarized in Figure 8, which shows the dispersion of multiphoton absorption cross-sections $\sigma^{(2)}$ and $\sigma^{(3)}$ (filled and empty squares, respectively) against the one-photon absorption spectra plotted as a function of doubled and tripled wavelength (grey solid and dashed lines, respectively). 3PA becomes dominant in the open aperture *f*-scan curves at 640 nm, which is shown in Figure 9(a) in the case of **E2-C$_8$-E2**. At wavelengths above 640 nm 2PA is no longer observed, whereas 3PA is clearly seen up to 825 nm, occurring in the spectral region which corresponds to the tripled wavelengths of the UV-Vis absorption region 225-275 nm. An example of open aperture curve featuring 3PA, measured in **E1-C$_8$-E1** solution at 800 nm, is presented in Figure 9(b).

The values of 3PA cross-sections were calculated directly from 3PA absorption coefficient of the solution (α_3), obtained by fitting open aperture data by 3PA theoretical curves based on the *f*-scan modification of the 3PA formula given by Gu *et al.*[38] It is also possible to calculate $\sigma^{(3)}$ from relation: $\sigma^{(3)} = E\sigma^{(2)}_{\text{eff}} / I_0$, where $\sigma^{(2)}_{\text{eff}}$ is the value of 2PA cross-section obtained from fitting the open aperture data by 2PA theoretical curves, $E = hc/\lambda$ is the photon energy and I_0 is the laser intensity obtained from closed aperture measurement of the silica reference. Such calculations give nearly the same values of $\sigma^{(3)}$. Each open aperture experimental curve at the wavelengths of 640 nm and above was fitted by both 2PA and 3PA, assuming contribution of only one of these phenomena during each fitting. Both $\sigma^{(3)}$ and effective $\sigma^{(2)}$ values were calculated in the spectral region dominated by 3PA, so that the relative strength of both optical limiting phenomena can be directly compared.

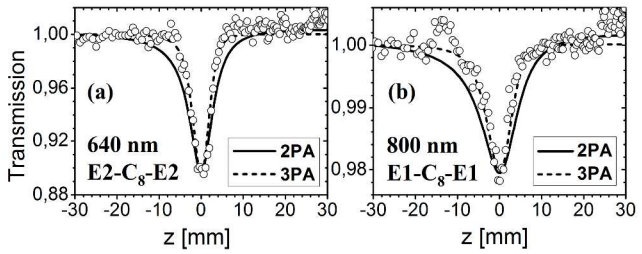

Figure 9. Examples of the open aperture *f*-scan curves revealing 3PA phenomenon.

Figure 8 reveals the spectral regions, where two different NLO absorption processes are simultaneously present, resulting in large error due to variations of the multiphoton cross sections obtained at a given wavelength under different laser intensities. Such effects are visible not only in 2PA values in the range of 600-680 nm, but also in the range of 850-950 nm, where another process – four-photon absorption (4PA) – is probably involved together with 3PA. Because the analysis of higher-order NLO

phenomena is associated with very large uncertainties, we refrain from going beyond 3PA. All of the open aperture curves obtained in our experiments above 640 nm are fitted separately by 2PA and 3PA theory, and possible contributions of higher-order absorption processes are accounted for by effective Im(γ) in Figure 6 (calculated from 2PA fits), and by effective cross sections $\sigma^{(2)}$ and $\sigma^{(3)}$ in Figure 8. These values are exact in the regions where only the one particular kind of nonlinear absorption is clearly dominant: $\sigma^{(2)}$ at 540-580 nm and $\sigma^{(3)}$ at 640-825 nm. Outside these regions they should be used only for indicative description of the optical limiting strength under assumption of a pure contribution of the given nonlinear absorption process. Continuation of the discussion on higher-order phenomena, including also the observation of higher-order nonlinear refraction, can be found in ESI.†

Conclusions

The investigated compounds exhibit very strong negative third-order nonlinear refraction in the 540-580 nm spectral range, with peak values of Re(γ) in the order of -5 and -4 × 10^{-33} esu in compounds **E1-C$_8$-E1** and **E2-C$_8$-E2**, respectively, and -1.4 × 10^{-32} esu in compound **E3-C$_8$-E3**. In all compounds the nonlinear refraction is accompanied by two-photon absorption with maximum cross-sections $\sigma^{(2)}$ varying from ~100 GM in **E2-C$_8$-E2** up to ~200 GM in **E1-C$_8$-E1** and **E3-C$_8$-E3**, corresponding to Im(γ) between 2.5 and 4.5 × 10^{-34} esu. These results are comparable with the data for the compound PtC$_8$Pt in Ref. 24 where peak values of Re(γ) = -3.2 × 10^{-33} and Im(γ) = 7 × 10^{-34} esu were found in the vicinity of 580 nm, not very different from the values in the present report. The high values of |Re(γ)/Im(γ)| merit factor obtained for the studied compounds confirm the potential suitability of the polyyne structural motif for optical switching. At longer wavelengths the samples exhibit complex nonlinear absorption behaviour, involving various multiphoton phenomena, with three-photon absorption being a dominant process in the range of 640-825 nm, showing maximum cross-sections $\sigma^{(3)}$ at 640 nm in the order of 5 × 10^{-79} cm^{6}s^2 in **E2-C$_8$-E2**, and up to 1 × 10^{-78} cm^{6}s^2 in **E1-C$_8$-E1** and **E3-C$_8$-E3**. The present results suggest that polyynes remain very interesting group of organic compounds from the point of view of their NLO properties, especially that, apparently, even small molecules of such type – of molecular mass not exceeding 500 g/mol – can exhibit quite large values of the NLO parameters. Further investigation of these compounds, including spectrally resolved NLO measurements and theoretical analysis of the electronic transitions involved in the NLO mechanisms, such as presented in Ref. 36, may allow for rational design of the polyyne molecules suitable for photonic applications in the useful spectral regions.

Acknowledgements

RK and MS would like to acknowledge the financial support from the Foundation for Polish Science (WELCOME grant 'Organometallics in NanoPhotonics') and the National Science Centre Poland (NCN grant UMO-2013/10/A/ST4/00114). SS would like to thank the National Science Centre (Grant number UMO-2013/08/M/ST5/00942) for financial support.

Notes and references

[a] *Faculty of Chemistry, University of Wroclaw, Joliot-Curie 14, Wroclaw 50-383, Poland. Tel: +4871 375 7122; fax: +4871 3282348; E-mail: slawomir.szafert@chem.uni.wroc.pl*

[b] *Advanced Materials Engineering and Modelling Group, Faculty of Chemistry, Wroclaw University of Technology, Wybrzeze Wyspianskiego 27, 50-370 Wroclaw, Poland, Tel:+48713204466; fax: +48713203364; E-mail: Marek.Samoc@pwr.edu.pl*

[c] *Laboratoire de Photonique Quantique et Moléculaire, École Normale Superieure de Cachan, 61 Avenue du Président Wilson, 94230 Cachan, France*

† Electronic Supplementary Information (ESI) available: [preparation, NMR spectra, X-ray details and higher order NLO effects]. See DOI: 10.1039/b000000x/

1 F. Cataldo, Polyynes: Synthesis Properties and Applications. CRC Press Taylor & Francis Group: Boca Raton, 2006; b) R. J. Lagow, J. J. Kampa, H.-Ch. Wei, S. L. Battle, J. W. Genge, D. A. Laude, C. J. Harper, R. Bau, R. C. Stevens, J. F. Haw, E. Munson, *Science*, 1995, **267**, 362–367.

2 a) S. Szafert, J. A. Gladysz, *Chem. Rev*., 2003, **103**, 4175–4205; b) S. Szafert, J. A. Gladysz, *Chem. Rev.,* 2006, **106**, PR1–PR33.

3 F. Cataldo, *Polym. Int.*, 1997, **44**, 191–200.

4 F. Diederich, P. J. Stang, R. R. Tykwinski, Acetylene Chemistry; Chemistry, Biology and Materials Science, Wiley-VCH: Weinheim, 2005.

5 a) K. West, C. Wang, A. S. Batsanov, M. R. Bryce, *Org. Biomol. Chem.*, 2008, **6**, 1934–1937; b) A. Ricci, M. Chiarini, C. Lo Sterzo, R. Pizzoferrato, S. Paoloni, *J. Photochem. Photobiol. A*, 2014, **298**, 1–8.

6 B. J. Cornil, D. Beljonne, J.-P. Calbert, J.-L. Bredas, *Adv. Mater.*, 2001, **13**, 1053–1067.

7 A. Sun, J. W. Lauher, N. S. Goroff, *Science*, 2006, **312**, 1030–1034.

8 G. Eres, C. M. Rouleau, M. Yoon, A. A. Puretzky, J. J. Jackson, D. B. Geohegan, *J. Phys. Chem. C,* 2009, **113**, 15484–15491.

9 C. Glaser, *Ber. Dtsch. Chem. Ges.* 1869, **2**, 422–424.

10 S. M. E. Simpkins, M. D. Weller, L. R. Cox, *Chem. Commun*., 2007, **30**, 4035–4037.

11 M. Gulcur, P. Moreno-Garcia, X. Zhao, M. Baghernejad, A. S. Batsanov, W. Hong, M. R. Bryce, T. Wandlowski, *Chem. Eur. J*., 2014, **20**, 4653–4660.

12 T. Gibtner, F. Hampel, J.-P. Gisselbrecht, A. Hirsch, *Chem. Eur. J.,* 2002, **8**, 408–432.

13 W. A. Chalifoux, R. R. Tykwinski, *Nature Chemistry*, 2010, **2**, 967–971.

14 a) W. Mohr, J. Stahl, F. Hampel, J. A. Gladysz, *Chem. Eur. J*., 2003, **9**, 3324–3340; b) N. J. Long, C. K. Williams*, Angew. Chem. Int. Ed*., 2003, **42**, 2586–2617: c) T. Bartik, B. Bartik, M. Brady, R. Dembinski, J. A**.** Gladysz, *Angew. Chem. Int. Ed. Engl.*, 1996, **35**, 414–417; d) R. Dembinski, T. Bartik, B. Bartik, M. Jaeger, J. A. Gladysz, *J. Am. Chem. Soc*., 2000**, 122**, 810–822.

15 Z. Cao, B. Xi, D. Jodoin, L. Zhang, S. P. Cummings, Y. Gao, S. F. Tyler, P. E. Fanwick, R. J. Crutchley, T. Ren, *J. Am. Chem. Soc.*, 2014, **136**, 12174–12183.

16 S. Eisler, A. D. Slepkov, E. Elliott, T. Luu, R. McDonald, F. A. Hegmann, R. R. Tykwinski, *J. Am. Chem. Soc*., 2005, **127**, 2666–2676.

17 A. D. Slepkov, F. A. Hegmann, S. Eisler, E. Elliott, R. R. Tykwinski, *J. Chem. Phys.* 2004, **120**, 6807-6810.

18 J.-W. Song, M. A. Watson, H. Sekino, K. Hirao, *J. Chem. Phys.* 2008, **129**, 024117-1-8.

19 B. B. Frank, P. R. Laporta, B. Breiten, M. C. Kuzyk, P. D. Jarowski, W. B. Schweizer, P. Seiler, I. Biaggio, C. Boudon, J.-P. Gisselbrecht, F. Diederich, *Eur. J. Org. Chem.,* 2011, 4307-4317.

20 J.-W. Song, M. A. Watson, H. Sekino, K. Hirao, *Int. J. Quantum Chem.,* 2009, **109**, 2012-2022.

21 T. Luu, E. Elliott, A. D. Slepkov, S. Eisler, R. McDonald, F. A. Hegmann, R. R. Tykwinski, *Org. Lett.,* 2005, **7**, 51-54.

22 G.-L. Xu, C.-Y. Wang, Y.-H. Ni, T. G. Goodson III, T. Ren, *Organometallics,* 2005, **24**, 3247-3254.
23 E. Fazio, L. D'Urso, G. Consiglio, A. Giuffrida, G. Compagnini, O. Puglisi, S. Patanè, F. Neri, G. Forte *J. Phys. Chem. C*, 2014, **118**, 28812-28819.
24. M. Samoc, G. T. Dalton, J. A. Gladysz, Q. Zheng. Y, Velkov, H. Ågren, P. Norman, M. G. Humphrey, *Inorg. Chem*., 2008, **47**, 9946–9957.
25 R. Kolkowski, M. Samoc, *J. Opt.,* 2014, **16**, 125202.
26 G. M.Sheldrick, *Acta Crystallogr. A*, 2008, **64**, 112–122.
27 M. Sheik-Bahae, A. A. Said, T.-H. Wei, D. J. Hagan, E. W. Van Stryland, *J. Quantum Electron.*, 1990, **26**, 760–769.
28 J. G. Breitzer, D. D. Dlott, L. K. Iwaki, S. M. Kirkpatrick, T. B. Rauchfuss, *J. Phys. Chem. A*, 1999, **103**, 6930-6937.
29 W. Chodkiewicz, *Ann. Agric. Sci. Ann. Chim., Paris* 1957, **2**, 819–869.
30 A. Hay, *J. Org. Chem.*, 1962, **27**, 3320–3321.
31 N. Gulia, K. Osowska, B. Pigulski, T. Lis, Z. Galewski, S. Szafert, *Eur. J. Org. Chem.*, 2012, 4819–4830.
32 I. Deperasinska, A. Szemik-Hojniak, K. Osowska, M. Rode, A. Szczepanik, Ł. Wiśniewski, T. Lis, S. Szafert*, J. Photochem. Photobiol. A*, 2011, **217**, 299–307.
33 B. F. Coles, P. B. Hitchcock, D. R. M. Walton, *J. Chem. Soc., Dalton Trans*., 1975, 442-445.
34 a) G. Wegner, *Z. Naturforsch. B,* 1969, **24**, 824–832; b) U. H. F. Bunz, Y. Rubin, Y. Tobe, *Chem. Soc. Rev.,* 1999, **28**, 107–119; c) F. Diederich, Y. Rubin, *Angew. Chem.,* 1992, **104**, 1123-1146; *Angew. Chem. Int. Ed. Engl.,* 1992, **31**, 1101–1123; d) R. R. Tykwinski, Y. Zhao, *Synlett,* 2002, 1939–1953; e) Y. Xu, M. D. Smith, M. F. Geer, P. J. Pellechia, J. C. Brown, A. C. Wibowo, L. S. Shimizu, *J. Am. Chem. Soc.,* 2010, **132**, 5334–5335; f) J. Xiao, M. Yang, J. W. Lauher, F. W. Fowler, *Angew. Chem.,* 2000, **112**, 2216-2219; *Angew. Chem. Int. Ed.,* 2000, **39**, 2132–2135; g) Y. Takeoka, K. Asai, M. Rikukawa, K. Sanui, *Chem. Commun.* 2001, 2592–2593; h) V. Enkelmann, *Chem. Mater.,* 1994, **6**, 1337–1340; i) V. Enkelmann, *Adv. Polym. Sci.,* 1984, **63**, 91–136; j) J. L. Foley, L. Li, D. J. Sandman, M. J. Vela, B. M. Foxman, R. Albro, C. J. Eckhardt, *J. Am. Chem. Soc.,* 1999, **121**, 7262–7263 and references cited therein; k) F. Carré, N. Devylder, S. G. Dutremez, C. Guérin, B. J. L. Henner, A. Jolivet, V. Tomberli, F. Dahan, *Organometallics,* 2003, **22**, 2014–2033; l) H. Irngartinger, M. Skipinski, *Tetrahedron,* 2000, **56**, 6781–6794; m) J. R. Neabo, K. I. S. Tohoundjona, J. F. Morin, *Org. Lett.,* 2011, **13**, 1358–1361; n) S. R. Diegelmann, N. Hartman, N. Markovic, J. D. Tovar, *J. Am. Chem. Soc.,* 2012, **134**, 2028–2031; o) Y. Nemoto, M. Sano, *J. Phys. Chem. B,* 2011, **115**, 12744–12750; p) J. Nagasawa, M. Yoshida, N. Tamaoki, *Eur. J. Org. Chem.,* 2011, 2247–2255.
35 M. Samoc, A. Samoc, B. Luther-Davies, Z. Bao, L. Yu, B. Hsieh, U. Scherf, *J. Opt. Soc. Am. B*, 1998, **15**, 817–825.
36 a) M. Sun, J. Chen, H. Xu, *J. Chem. Phys.,* 2008, **128**, 064106-1-8.; b) J. Liu, J. Xia, P. Song, Y. Ding, Y. Cui, X. Liu, Y. Dai, F. Ma, *Chem. Phys. Chem.,* 2014, **15**, 2626-2633.
37 B. Luther-Davies and M. Samoc, *Curr. Opin. Solid State Mater. Sci.*, 1997, **2**, 213-219.
38 B. Gu, J. Wang, J. Chen, Y.-X. Fan, J. Ding, H.-T. Wang, *Opt. Express,* 2005, **13**, 9230-9234.